SAND2014-16367J

Evaluation of Global Horizontal Irradiance to Plane of Array Irradiance Models at Locations across the United States

Matthew Lave, *Member, IEEE,* William Hayes, Andrew Pohl, and Clifford W. Hansen

***Abstract*—We report an evaluation of the accuracy of combinations of models that estimate plane-of-array (POA) irradiance from measured global horizontal irradiance (GHI). This estimation involves two steps: (1) decomposition of GHI into direct and diffuse horizontal components; and (2) transposition of direct and diffuse horizontal irradiance to POA irradiance. Measured GHI and coincident measured POA irradiance from a variety of climates within the United States were used to evaluate combinations of decomposition and transposition models. A few locations also had diffuse horizontal irradiance (DHI) measurements, allowing for decoupled analysis of either the decomposition or the transposition models alone. Results suggest that decomposition models had mean bias differences (modeled versus measured) that vary with climate. Transposition model mean bias differences depended more on the model than the location. When only GHI measurements were available and combinations of decomposition and transposition models were considered, the smallest mean bias differences were typically found for combinations which included the Hay/Davies transposition model.**

I. Introduction

MODELS which estimate plane-of-array (POA) irradiance from measured global horizontal irradiance (GHI) are critical to PV performance analysis because often only GHI measurements are available whereas the PV modules being analyzed are tilted to maximize annual insolation. Modeling POA irradiance from GHI involves two steps: (1) the decomposition of GHI into its direct and diffuse components, usually expressed as diffuse horizontal irradiance (DHI) and direct normal irradiance (DNI), and (2) the transposition of these components to POA of the modules. No combination of decomposition and transposition models is widely accepted as a standard for converting GHI to POA; various pairs of decomposition plus transposition models are in use. This lack of consistency leads to different predictions of POA irradiance, even when using the same input GHI. For example, Fig. 1 shows that performance estimated using the program PVsyst [1] can vary by over 1% simply by changing the transposition model from Hay/Davies [2] to Perez [3].

Sandia National Laboratories is a multi-program laboratory managed and operated by Sandia Corporation, a wholly owned subsidiary of Lockheed Martin Corporation, for the U.S. Department of Energy's National Nuclear Security Administration under contract DE-AC04-94AL85000.

M.Lave is with the Sandia National Laboratories, Livermore, CA, 94550, USA (e-mail: mlave@sandia.gov).

W. Hayes is with First Solar, San Francisco, CA, 94105, USA.

A. Pohl and C. Hansen are with Sandia National Laboratories, Albuquerque, NM, 87185, USA.

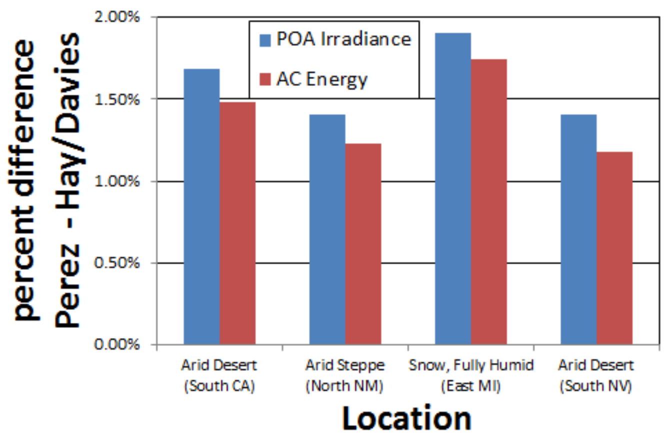

Fig. 1. Annual differences in POA irradiance and AC energy between the Perez and Hay/Davies transposition models as implemented in PVsyst.

There are numerous previous works evaluating either decomposition models (e.g., [4], [5]), transposition models (e.g., [6], [7], [8]), or combinations of both (e.g., [9]). However, most of these evaluations compare models with data at a single location (Ineichen [4] is a notable exception as 22 locations across the world were used to test decomposition models), and most do not go beyond simple annual metrics such as root mean squared difference (RMSD) or mean bias difference (MBD). Here, we evaluate the performance of decomposition models and transposition models separately, as well as combinations of decomposition with transposition models, at a variety of locations across the United States. Our work builds upon previous studies because we analyze each model's performance over many different test climates and we examine model performance in greater detail; for example, we consider decomposition model errors as a function of clearness index, the relationship between the bias in model combinations and the biases in the separate decomposition and transposition models, and the potential for redundant sensors to reduce the effect of sensor bias on the analysis.

II. Models

Figure 2 shows how the transposition model, or the combination of a decomposition and a transposition model, are used to estimate POA irradiance from available measurements. We discuss the specific models we considered in our analysis in the following subsections.

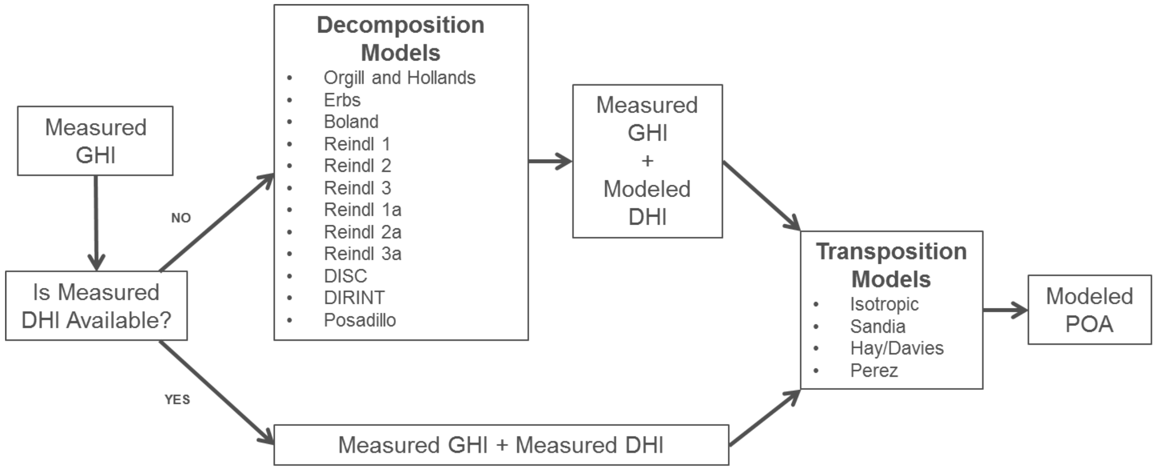

Fig. 2. Flowchart showing how to model POA irradiance from measured GHI.

A. Decomposition Models

We consider the decomposition models listed in Table I. All models are empirical, in that their equations are not formally derived from physical laws but rather involve coefficients that were estimated from a fixed set of measured data at one or a handful of locations. We refer the reader to the references in Table I for detailed model descriptions. Note that Reindl [10] proposes three different models of increasing complexity (termed here Reindl 1, Reindl 2, and Reindl 3) depending on the available input data. Additionally, the performance of the Reindl models during times of high clearness index may be improved by adjusting the bound between two of the clearness index intervals [11]. The Reindl models with this adjusted interval are referred to as the Reindl adjusted models. Specifically, in the Reindl adjusted models, the intervals in equations 2b, 3b, and 4b in [10] are changed to $0.3 < k_t < 0.83$ and the intervals in equations 2c, 3c, and 4c are changed to $0.83 < k_t$.

TABLE I
DECOMPOSITION MODELS.

Model	Input variables	Abbreviation
Orgill and Hollands [12]	Kt, GHI	OH
Erbs [13]	Kt, GHI	Er
Boland [14]	Kt, GHI	Bo
Reindl 1 [10]	Kt, GHI	R1
Reindl 1 adj	Kt, GHI	R1a
DISC [15]	Kt, GHI, $SunEl$	DIS
DIRINT [16]	Kt, GHI, $SunEl$	DIR
Reindl 2 [10]	Kt, GHI, $SunEl$	R2
Reindl 2 adj	Kt, GHI, $SunEl$	R2a
Reindl 3 [10]	Kt, GHI, $SunEl$, $AmbT$, RH	R3
Reindl 3 adj	Kt, GHI, $SunEl$, $AmbT$, RH	R3a
Posadillo [17]	Kt, GHI, $SunEl$, MF	Po

All decomposition models use at least the clearness index Kt and GHI as inputs. Many models also account for the solar elevation angle $SunEl$. The Reindl 3 models use the ambient temperature $AmbT$ and the relative humidity RH, while the Posadillo model uses a modulating function MF based on the 5-minute variability in GHI.

The explicit output of most decomposition models is DHI, though some models produce DNI instead. Because DHI and DNI are related by:

$$DNI = \frac{GHI - DHI}{sin(SunEl)}, \tag{1}$$

all decomposition models effectively produce estimates of both DHI and DNI.

B. Transposition Models

Table II lists the transposition models we evaluate. The models determine total POA irradiance by estimating the direct, ground reflected diffuse, and sky diffuse components on the plane of array:

$$POA = POA_{dir} + POA_{diff,refl} + POA_{diff,sky}. \tag{2}$$

TABLE II
TRANSPOSITION MODELS.

Model	Input variables
Isotropic [18]	$SurfTilt$, DHI
Sandia (King) [19]	$SurfTilt$, DHI, GHI, $SunEl$
Hay/Davies [2]	$SurfTilt$, $SurfAz$, DHI, DNI, $HExtra$, $SunEl$, $SunAz$
Perez [3]	$SurfTilt$, $SurfAz$, DHI, DNI, $HExtra$, $SunEl$, $SunAz$, AM

The direct irradiance incident on the POA, POA_{dir}, can be calculated directly from DNI through geometric relations:

$$POA_{dir} = DNI \times cos(AOI) \tag{3}$$

where AOI is the angle of incidence of the sun beam on the POA surface.

The ground reflected diffuse irradiance is typically estimated as a simple function of GHI, ground albedo (ρ), and the surface tilt from horizontal (β):

$$POA_{diff,refl} = GHI \times \rho \times \frac{1 - cos(\beta)}{2} \tag{4}$$

All transposition models we consider, except for the Sandia model, use Eqn. 4, and we assume $\rho = 0.2$ for all. The

Sandia transposition model uses an albedo equation that was empirically fit to data from Albuquerque, NM.

The transposition models vary in their estimation of the sky diffuse irradiance on the POA, $POA_{diff,sky}$. The models range from the simple assumption that diffuse POA irradiance depends only on the amount of sky 'seen' by the surface (e.g., the isotropic and Sandia models) to complicated empirical relationships with multiple look-up tables (e.g., the Perez model).

III. Data Description

Details about the data at each location are shown in Table III, and the station locations are mapped in Fig. 3. Data for stations 1-6 was contributed by First Solar, Inc., and GHI and POA measurements were taken using Kipp & Zonen CMP 11 secondary standard pyranometers. Stations 3 and 4 also included DHI measurements using Irradiance, Inc. Rotating Shadowband Radiometers which rely on Licor first class pyranometers. Data for Station 9 was contributed by Southern Company, and Licor first class pyranometers were used to measure GHI and POA irradiance. (Note that station numbering is not sequential due to the removal of two stations which did not have sufficient periods of record.) Station 10 is located in Golden, CO at NREL's Solar Radiation Research Laboratory [20]; the Global CM22 measurement from a secondary standard Kipp & Zonen CM22 was used for GHI, the Diffuse CM22 measurement also from a CM22 was used for DHI, and the Global 40-South PSP measurement from a first class Eppley Precision Spectral Pyranometer (PSP) was used for POA irradiance. Stations 11 (Livermore, CA) and 12 (Albuquerque, NM) are operated by Sandia National Laboratories. Station 11 uses Eppley PSPs for GHI and DHI measurements, but does not have a POA measurement. Station 12 uses Eppley PSPs for both GHI and POA measurements.

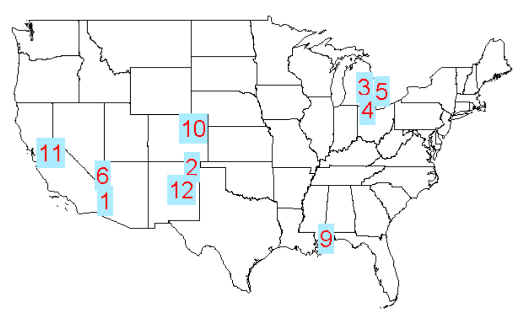

Fig. 3. Map of station locations.

For all stations except Station 9, data were available for one year or more. In these cases, we used only year-long periods of data (e.g., 1-year, 2-years, etc.) even though longer periods of record were available to ensure equal weighting of seasonal effects. At Station 9, only 10 months of data were available. We choose to include Station 9 in our analysis, but caution that winter effects may not be fully captured. All data were collected at a resolution of one minute. POA measurements were collected at due south azimuth, which is consistent with the majority of installed solar PV modules, but limits this analysis to south-oriented fixed tilt systems. Stations 10 and 12 are at high altitude.

The stations equipped with DHI measurements (Stations 3, 4, 10, 11, 12) allowed for analysis of the decomposition models separately. The stations with both DHI and POA measurements (Stations 3, 4, 10, 12) allowed for separate analysis of the transposition models.

IV. Analysis

Three distinct analyses were undertaken: (A) decomposition models alone using measured GHI as input and compared to measured DHI, (B) transposition models alone using measured DHI as input and compared to measured POA, and (C) combinations of decomposition and transposition models using measured GHI as input and compared to measured POA. In this last case, DHI estimated from the decomposition models was input to the transposition models.

We first summarize all measured data to hourly averages because the considered models were designed to predict hourly values of their output quantities. Since errors in measurements may contribute to model errors in our analysis, we use the term differences rather than errors when comparing modeled to measured data. Measurement bias errors are difficult to distinguish from model bias errors, and may influence our analysis. We attempt to minimize the effect of measurement bias on our conclusions by evaluating the performance of the combined models using colocated pairs of GHI and POA sensors in section IV-C.

Simple quality control metrics were applied to all data. All GHI, DHI, and POA values less than 0 Wm^{-2} or greater than 2000 Wm^{-2} were removed from the analysis, since these values were likely erroneous measurements. Additionally, any DHI measurement that exceeded the concurrent GHI measurement was set equal to the GHI measurement because it is not physically possible for DHI to exceed GHI. In these few situations, DHI only slightly exceeded GHI – the difference was not large enough to warrant rejecting the DHI measurement as erroneous. At the few times when POA measurements were excessively greater than GHI measurements (e.g., the POA measurement indicated clear-sky while the GHI measurement indicated overcast conditions), data were removed because the values were likely a result of data collection errors.

Specific quality control was needed at some of the locations. At one location, shading was observed that occluded the GHI sensor but not the POA sensor; times at which this shading occurred were eliminated from the analysis. At Stations 3 and 4, inconsistencies were found between the CMP11 measured GHI and the RSR/Licor measured GHI. We chose to use the CMP11 instrument because it is a higher standard (secondary standard), however, DHI measurements were only available from the RSR/Licor. Thus, we computed the diffuse fraction ($\frac{DHI_{RSR}}{GHI_{RSR}}$) using the RSR/Licor measurements, and then multiplied the CMP11-measured GHI by this diffuse fraction to obtain the DHI at Stations 3 and 4.

TABLE III
DATA LOCATIONS AND CLIMATES.

Station	Location	Elevation [m]	Climate Zone	Measured Data	Time Period	*SurfTilt*	*SurfAz*
1	Southeast CA	120	Arid Desert Hot (BWh)	GHI, POA	1/2010 - 12/2012	25°	180°
2	Northeast NM	100	Arid Steppe Cold (BSk)	GHI, POA	1/2012 - 12/2012	25°	180°
3	East MI	188	Snow; Fully humid; Warm summer (Dfb)	GHI, DHI, POA	8/2012 - 7/2013	25°	180°
4	East MI	181	Snow; Fully humid; Warm summer (Dfb)	GHI, DHI, POA	8/2012 - 7/2013	25°	180°
5	East MI	193	Snow; Fully humid; Warm summer (Dfb)	GHI, POA	10/2010 - 9/2013	25°	180°
6	Southern NV	572	Arid Desert Hot (BWh)	GHI, POA	1/2011 - 12/2012	25°	180°
9	Coastal MS	6	Warm temperate; Fully humid; Hot summer (Cfa)	GHI, POA	2/2013 - 11/2013	15°	180°
10	Central CO	1829	Arid Steppe Cold (BSk)	GHI, DHI, POA	1/2013 -12/2013	40°	180°
11	Central CA	200	Warm temperate; dry, hot summer (CSa)	GHI, DHI	1/2013 -12/2013	N/A	N/A
12	Central NM	1657	Arid Steppe Cold (BSk)	GHI, DHI, POA	1/2011 12/2011	35°	180°

A. *Decomposition Models*

Relative accuracy of the decomposition models (modeled DHI compared to measured DHI) was evaluated for the 5 stations with DHI measurements (Stations 3, 4, 10, 11, and 12). Figure 4 shows the relative (% relative to GHI) Root Mean Squared Difference (rRMSD) and the relative Mean Bias Difference (rMBD) for each decomposition model and each station. These metrics quantify the average (over time) differences between modeled and measured data: rRMSD relates to the differences in hourly values and rMBD relates to the annual difference.

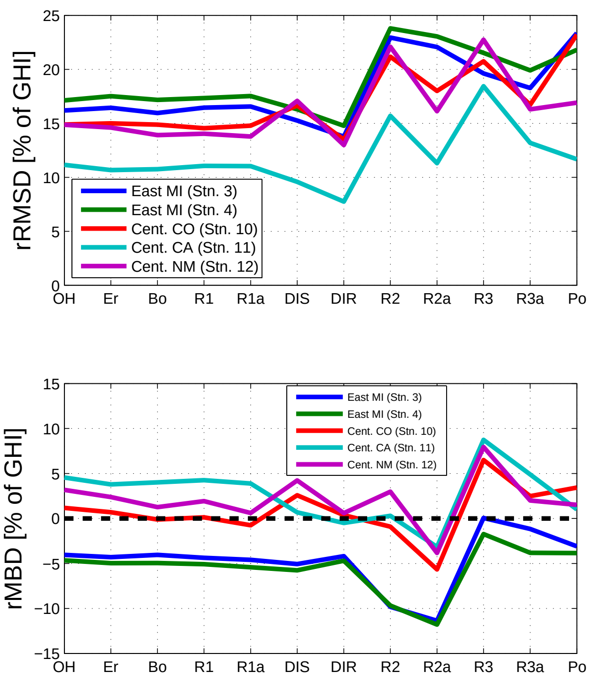

Fig. 4. Relative (to GHI) root mean squared (rRMSD) and mean bias (rMBD) differences (modeled minus measured) for each of the 12 decomposition models (x-axis) at each of the five stations with DHI measurements.

Model performance is similar across all stations for the 'simple' decomposition models which only use Kt and GHI as inputs (Orgill and Hollands, Erbs, Boland, Reindl 1, and Reindl 1a): these models have between 11-17% rRMSD. The rMBDs do not show this same consistency, as they range from -5% to +5% between stations, although at the same station all simple models have similar performance. Both the relative similarity of rRMSDs across locations and the variation of rMBD by location is in agreement with the findings of [4].

The rMBD differences by location were at least partly due to climate differences: the biases were negative for the cloudier eastern Michigan stations and were positive for the clearer Livermore and Albuquerque stations (again consistent with [4] who generally found negative bias errors in DNI models at clear locations). The simple decomposition models typically under-predict DHI during cloudy periods and over-predict DHI during clear periods.

Fig. 5 shows the errors in the Erbs model plotted as a function of the measured clearness index and diffuse fraction, and the rMBD as a function of clearness index. During partly cloudy periods, the Erbs model underestimates the DHI (dark colors in Fig. 5). The dominance of partly cloudy conditions at Station 3 (i.e., points falling above the black dashed line in Fig 5) causes a negative bias in the Erbs model. Conversely, during clear periods the Erbs model overestimates DHI (light colors in Fig. 5). At Station 11, the many clear periods (i.e., the collection of points around measured clearness index $Kt = 0.75$, measured diffuse fraction $DF = 0.1$) lead to a positive bias in the Erbs model.

Nearly identical biases were observed in all simple decomposition models. The more complicated decomposition models showed the same overall trends — underestimating DHI in cloudy locations and overestimating DHI in clear locations — but bias analysis was more complicated due to the additional input variables used by the models.

At all locations, the DIRINT model had the smallest rRMSD and rMBD. However, the performance of the simple models was not significantly worse. Consequently, we focused our analysis of model combinations on those involving either the DIRINT model, because it shows the best performance, or the Erbs model, because it is representative of the simple models and is the default decomposition model in PVsyst.

B. *Transposition Models*

Using measured DHI values at stations 3, 4, 10, and 12 the relative accuracy of the different transposition models was evaluated. Fig. 6 shows the rRMSDs and rMBDs.

With the exception of the Sandia model, the model biases were relatively consistent across the different locations. The isotropic model always produced the lowest POA estimates since it does not add any enhanced diffuse irradiance in the circumsolar region. The albedo correction that the Sandia

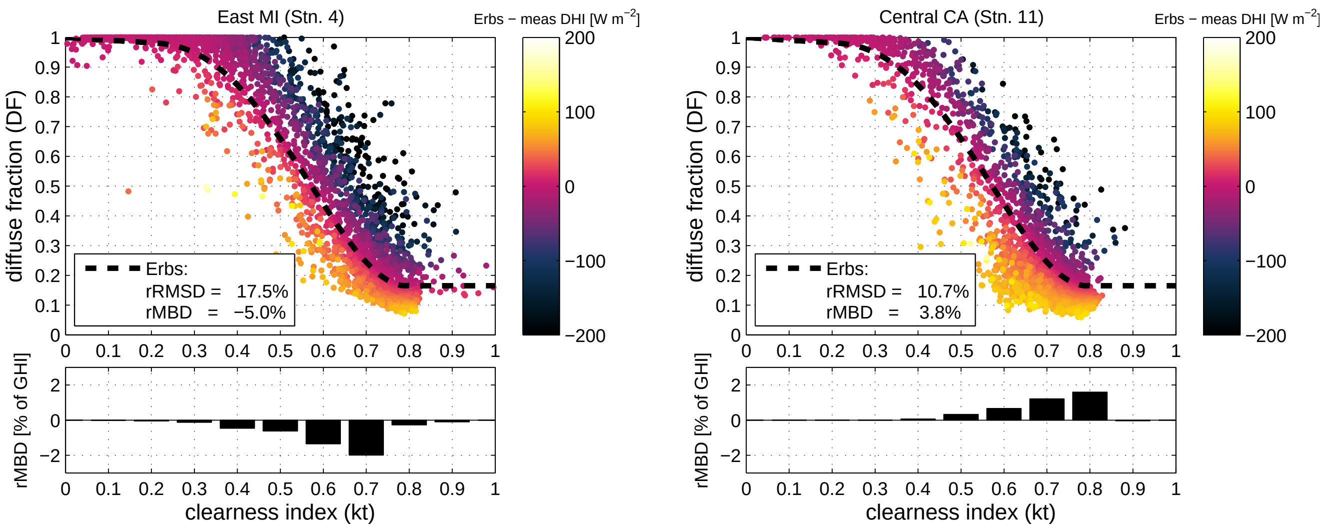

Fig. 5. [Top plots] Hourly differences (colors) in Erbs modeled minus measured DHI, plotted as a function of measured clearness index (x-axis) and measured diffuse fraction (y-axis). The black dashed line is the Erbs modeled diffuse fraction as a function of clearness index. [Bottom plots] Relative (to GHI) mean bias differences plotted as a function of clearness index.

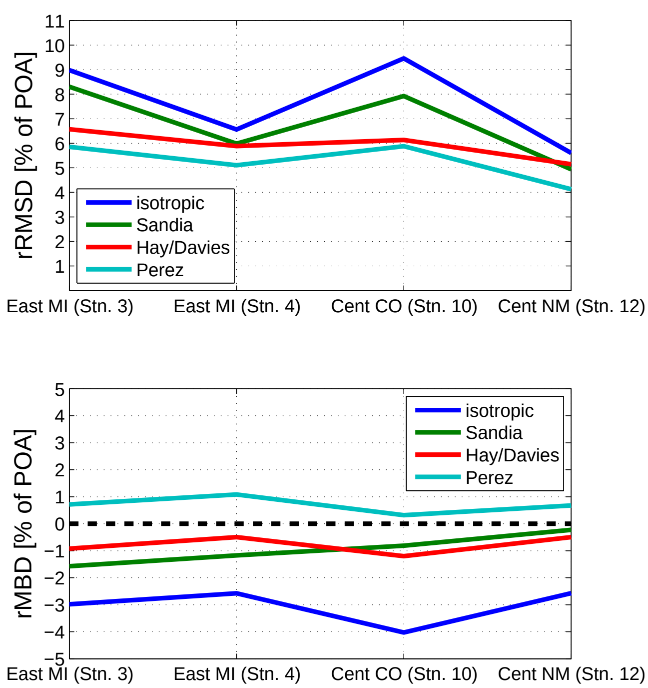

Fig. 6. Relative (to POA) root mean squared (RMSD) and mean bias (MBD) differences modeled versus measured for each of the 4 transposition models at each of the 4 stations with DHI and POA measurements.

model applies to the isotropic model caused the Sandia model to always have larger POA estimates than the isotropic model. The Sandia model had the lowest rMBD at the Station 12, as expected due to the model being calibrated using data at this location. rRMSDs were larger for the isotropic and Sandia models than for the Hay/Davies and Perez models.

Both the Hay/Davies and Perez models produced rMBDs that were smaller than 1.5% at all locations. The Perez model always estimated 1 to 2% more annual POA irradiance than the Hay/Davies model, consistent with the analysis run in PVsyst shown in Fig. 1. The Perez transposition model has the smallest rRMSD at all locations, indicating it may be the best model choice when measured DHI is available. However, the Hay/Davies model results in only slightly increased rRMSD. For combination models, we will focus on the Hay/Davies and Perez transposition models.

C. Combined Models

We focused our analysis on model combinations which involved the two best performing decomposition (Erbs and DIRINT) and transposition models (Hay/Davies and Perez), resulting in four combined models. The rRMSDs and rMBDs of these combined models are shown in Fig. 7. For comparison, the transposition models run with measured DHI are included as dots in Fig 7.

The same order of transposition model rMBD (Perez $>$ Hay/Davies) is observed. In the combined model case, however, all combinations tend to overestimate annual irradiance, meaning that combinations involving the Perez transposition model are now even more positively biased than noted in the transition model with measured DHI case. The DIRINT plus Hay/Davies model combination typically had the smallest rMBDs, though the Erbs plus Hay/Davies combination had only slightly larger rMBDs. The rRMSDs change more with changing station than with changing model. Although the rMBDs are rather consistent across Stations 2-6 ($\sim$1% for combinations involving Hay/Davies and $\sim$2% for combinations involving Perez), the rRMSDs vary widely across those locations (from $<$5% to over 10%).

This initial analysis of the combined models inspired two further investigations: (1) how the individual decomposition and transposition model biases related to the combined model

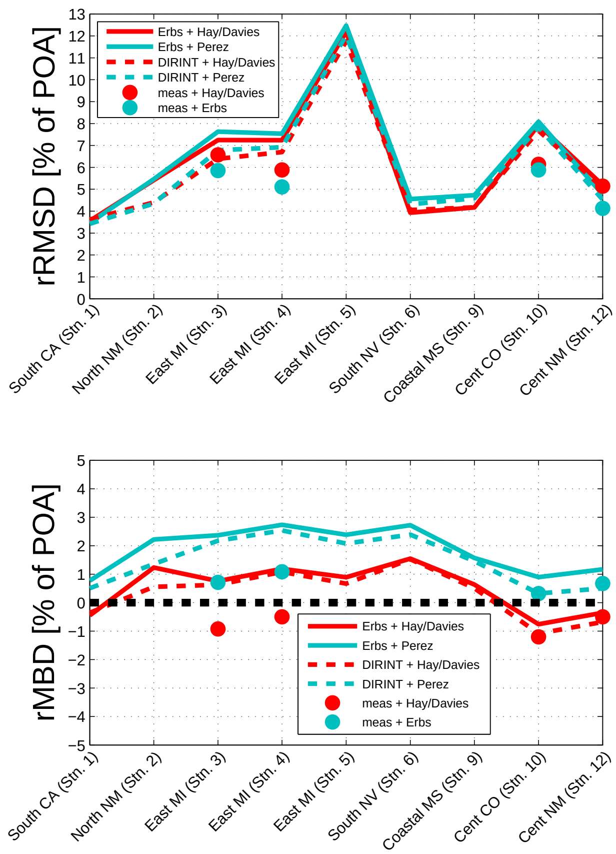

Fig. 7. Relative (to POA) root mean squared (rRMSD) and mean bias differences (rMBD) for combinations of decomposition and transposition models. Also included (as dots) are the rRMSDs and rMBDs for the transposition models with measured DHI.

biases (2) how bias errors in measurements may be affecting our combined model analysis results.

1) Relationship between Combined and Individual Model Biases: In the results shown in Fig. 7, the rMBDs at Stations 3 and 4 (cloudy locations) were more positive for the combined models than for the transposition models with measured DHI. This is expected since both the Erbs and DIRINT models underestimated DHI (Fig. 4), and when the decomposition models underestimate DHI, they inherently overestimate DNI (since DNI and DHI are related by Eq. 1). A larger DNI estimate then typically leads to a larger POA irradiance estimate since the POA is usually chosen to maximize direct (and hence annual) irradiance.

However, while both the Erbs and the DIRINT models had positive errors at Station 12 (+2.4% and +1.5%, respectively), suggesting a decrease in POA irradiance, the rMBD was practically unchanged for the combined models from the transposition model with measured case. The Erbs with Perez model actually leads to an increase in the POA irradiance.

Fig. 8 shows the relationship between decomposition model bias, transposition model bias, and combined model bias by plotting these rMBDs for all model combinations at Stations 3, 4, 10, and 12. It is expected that POA biases will increase moving to the left (decreasing DHI and hence increasing DNI estimates from decomposition models) and up (increasing POA estimates from the transposition models) in Fig. 8, and, indeed, for the most part this gradient was observed. However, some notable exceptions occur. Almost all model combinations involving the Perez transposition had positive biases, even when the decomposition models had positive biases. The isotropic model appears to be insensitive to small decomposition errors: model combinations including the isotropic model and a decomposition model with rMBD between -2% to +4% consistently had combined model rMBDs of 2.5% to 4%.

Deviations from the expected gradient (increasing combined model bias with decreasing decomposition model bias and increasing transposition model bias) are likely due to hourly deviations in the decomposition or transposition models which are not fully resolved with the rMBD metric. Due to the complicated dependencies of each model, biases in the decomposition models may be either minimized or amplified by the transposition models. Thus, biases in the individual models may suggest but do not necessarily determine the biases of the combined models. Based on the results shown in Figs. 7 and 8, combined models involving Hay/Davies appear to have less bias than combined models involving Perez, even though Hay/Davies and Perez had similar biases when using measured DHI.

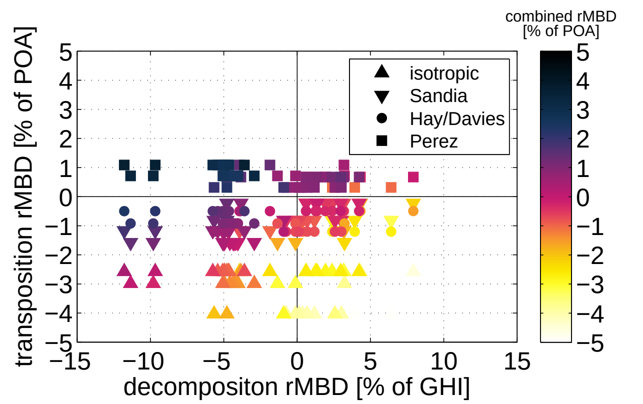

Fig. 8. Scatter plot of combined model rMBD (colors) plotted against the decomposition model and transposition model rMBDs. All 12 decomposition models and all 4 transposition models evaluated at Stations 3, 4, 10, and 12 are included in this plot.

2) Influence of Measurement Biases on Combined Model Findings: While it appears that model combinations involving Hay/Davies are less biased, our results could be influenced by measurement biases (e.g., a positive sensor bias may incorrectly make the models appear biased negative). We attempted to reduce the effect of sensor bias by looking at multiple pairs of GHI and POA sensors at the same location. For example, there were 6 GHI and 6 POA sensors at Station 5, so we evaluated the combined model biases using all 36 possible GHI-POA combinations. If all sensors considered had some measurement bias, but the mean of all measurement biases was close to zero, then this method will reduce the impact of measurement bias.

A box plot describing the distribution of rMBDs of the combined models using the 77 different GHI-POA pairs available at Stations 1-6 is shown in Fig. 9. The widths of the

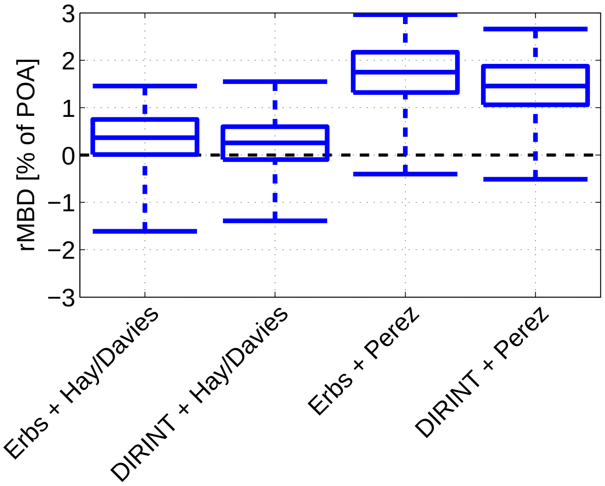

Fig. 9. Box plot of the combined model rMBD for 77 GHI-POA sensor pairs located at Stations 1-6.

distributions are around 3%, which is consistent with expected sensor uncertainties [21]. There may still be some biases that are the same among all GHI-POA sensor pairs, such as tilt-angle response, that were still affecting this analysis, but these are expected to be small (e.g., tilt angle response $< 0.2\%$ for CMP 11 [22]). Therefore, the median rMBD of all sensor pair combinations was likely close to the true rMBD since sensor biases were mostly removed.

The median rMBD was 0.5% for Erbs with Hay/Davies, 0.3% for DIRINT with Hay/Davies, 1.9% for Erbs with Perez, and 1.6% for DIRINT with Perez. Thus, when sensor error is minimized, the model combinations with the Hay/Davies transposition model continue to appear to be the least biased.

V. Conclusion

GHI to POA models were evaluated at a variety of locations across the United States. Decomposition models had different biases based on location, consistent with previous findings [4]. This was caused by the models often underestimating the diffuse irradiance at cloudy locations and overestimating the diffuse at clear locations. Transposition model performance did not vary much by location; at all locations the isotropic model produced the smallest POA estimate and the Perez model the largest. Based on root mean squared deviation, the Erbs and DIRINT decomposition models and the Hay/Davies and Perez transposition models were chosen as the best performing models and use for evaluation of combined model performance. Little difference was observed in the combined models whether DIRINT or Erbs was used for the decomposition model, but a large difference was seen between the model combinations involving the Hay/Davies versus the Perez transposition models. Model combinations involving the Hay/Davies transposition model appeared to have less bias than combinations involving the Perez transposition model, even though both Hay/Davies and Perez had similar bias magnitudes when using measured diffuse irradiance. Further analysis testing the impact of decomposition and transposition model bias on combined model bias and minimizing the effect of sensor error again suggested that combined models involving the Hay/Davies model led to smaller bias.

While this analysis has suggested that it may be best to use the Hay/Davies model when using a decomposition model to estimate diffuse irradiance, it also indicates that both decomposition and transposition models could be improved. Decomposition models could be modified to remove the locational dependence, possibly by using the clear-sky index which, as opposed to the clearness index, accounts for factors such as the atmospheric turbidity and station elevation. Further study of the circumsolar and other sky regions could enhance the transposition model performance. Additionally, transposition models could be modified to be less sensitive to deviations in diffuse irradiance, such that they have smaller biases when combined with decomposition models. Finally, transposition models were designed using fixed-tilt systems, but could be optimized for single- or two-axis tracking systems for broader application.

Acknowledgment

Thanks to William Hobbs at Southern Company for supplying the data from Station 9.

References

[1] A. Mermoud, "PVsyst," http://www.pvsyst.com/.
[2] J. Hay and J. Davies, "Calculations of the solar radiation incident on an inclined surface," in *Proc. of First Canadian Solar Radiation Data Workshop, 59*. Ministry of Supply and Services, Canada.
[3] R. Perez, R. Seals, P. Ineichen, R. Stewart, and D. Menicucci, "A new simplified version of the perez diffuse irradiance model for tilted surfaces," *Solar Energy*, vol. 39, no. 3, pp. 221–231, 1987.
[4] P. Ineichen, "Comparison and validation of three global-to-beam irradiance models against ground measurements," *Solar Energy*, vol. 82, no. 6, pp. 501 – 512, 2008. [Online]. Available: http://www.sciencedirect.com/science/article/pii/S0038092X07002551
[5] C. Jacovides, F. Tymvios, V. Assimakopoulos, and N. Kaltsounides, "Comparative study of various correlations in estimating hourly diffuse fraction of global solar radiation," *Renewable Energy*, vol. 31, no. 15, pp. 2492 – 2504, 2006. [Online]. Available: http://www.sciencedirect.com/science/article/pii/S0960148105003538
[6] P. G. Loutzenhiser, H. Manz, C. Felsmann, P. A. Strachan, T. Frank, and G. M. Maxwell, "Empirical validation of models to compute solar irradiance on inclined surfaces for building energy simulation," *Solar Energy*, vol. 81, no. 2, pp. 254–267, 2007.
[7] D. Wlodarczyk and H. Nowak, "Statistical analysis of solar radiation models onto inclined planes for climatic conditions of lower silesia in poland," *Archives of Civil and Mechanical Engineering*, vol. 9, no. 2, pp. 127 – 144, 2009. [Online]. Available: http://www.sciencedirect.com/science/article/pii/S1644966512600648
[8] A. M. Noorian, I. Moradi, and G. A. Kamali, "Evaluation of 12 models to estimate hourly diffuse irradiation on inclined surfaces," *Renewable Energy*, vol. 33, no. 6, pp. 1406 – 1412, 2008. [Online]. Available: http://www.sciencedirect.com/science/article/pii/S0960148107002509
[9] C. A. Gueymard, "Direct and indirect uncertainties in the prediction of tilted irradiance for solar engineering applications," *Solar Energy*, vol. 83, no. 3, pp. 432 – 444, 2009. [Online]. Available: http://www.sciencedirect.com/science/article/pii/S0038092X08002983
[10] D. T. Reindl, W. A. Beckman, and J. A. Duffie, "Diffuse fraction correlations," *Solar Energy*, vol. 45, no. 1, pp. 1–7, 1990.
[11] W. Hayes, personal communication, 2014.
[12] J. F. Orgill and K. G. T. Hollands, "Correlation equation for hourly diffuse radiation on a horizontal surface," *Solar Energy*, vol. 19, no. 4, pp. 357–359, 1977.
[13] D. G. Erbs, S. A. Klein, and J. A. Duffie, "Estimation of the diffuse radiation fraction for hourly, daily and monthly-average global radiation," *Solar Energy*, vol. 28, no. 4, pp. 293–302, 1982.
[14] J. Boland, B. Ridley, and B. Brown, "Models of diffuse solar radiation," *Renewable Energy*, vol. 33, no. 4, pp. 575–584, 2008.

[15] E. L. Maxwell, “A quasi-physical model for converting hourly global horizontal to direct normal insolation,” Solar Energy Research Institute, Tech. Rep., 1987.

[16] R. Perez, “Dynamic global to direct conversion models,” *ASHRAE Transactions Research Series*, pp. 154–168, 1992.

[17] R. Posadillo and R. López Luque, “Hourly distributions of the diffuse fraction of global solar irradiation in crdoba (spain),” *Energy Conversion and Management*, vol. 50, no. 2, pp. 223–231, 2009.

[18] B. Y. H. Liu and R. C. Jordan, “The interrelationship and characteristic distribution of direct, diffuse and total solar radiation,” *Solar Energy*, vol. 4, no. 3, pp. 1–19, 1960.

[19] D. King, “Simple sandia sky diffuse model.” [Online]. Available: http://pvpmc.org/modeling-steps/incident-irradiance/plane-of-array-poa-irradiance/calculating-poa-irradiance/poa-sky-diffuse/simple-sandia-sky-diffuse-model/

[20] National Renewable Energy Laboratory, “Measurement and instrumentation data center.” [Online]. Available: http://www.nrel.gov/midc

[21] T. Stoffel, “A review of measured/modeled solar resource uncertainty,” in *2013 Sandia PV Performance Modeling Workshop*, 2013.

[22] Kipp & Zonen, “Instruction manual cmp series pyranometer,” http://www.kippzonen.com/Download/72/Manual-Pyranometers-CMP-series-English, 2014.

Matthew Lave received the Ph.D. degree in aerospace engineering from the University of California, San Diego.

He is a Senior Member of the Technical Staff at Sandia National Laboratories, working in the Photovoltaic and Distributed Systems Integration Department. His specialty areas are solar resource assessment, PV performance monitoring, and grid integration of PV, especially related to large data set analysis. He currently develops and validates models of solar irradiance, spatial smoothing of solar variability across large PV plants, and the impact of PV to the electric grid.

William Hayes received the M.S. degree in mechanical engineering from the University of California, San Diego.

He is a member of the Performance and Prediction team at First Solar, Inc. His expertise lies in modeling the thermal response of operational PV modules in utility scale deployment. He currently models and evaluates the performance of utility scale PV system focusing on driving down the uncertainty in PV system energy estimates.

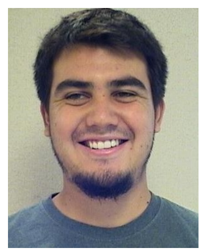

Andrew Pohl received the B.S. degree in applied mathematics from the University of New Mexico and is currently pursuing the M.S. degree in statistics also from the University of New Mexico.

He is a student intern at Sandia National Laboratories, working in the Photovoltaic and Distributed System Integration Department.

Clifford W. Hansen received the Ph.D. degree in mathematics from The George Washington University in Washington, D.C.

He is a Distinguished Member of the Technical Staff at Sandia National Laboratories, working in the Photovoltaics and Distributed Systems Integration Department. His research focuses on methods for PV system modeling, model calibration from component characterization, and uncertainty in estimates of the solar resource and PV system production.